Atmos. Chem. Phys. Discuss., 12, 5881–5901, 2012
www.atmos-chem-phys-discuss.net/12/5881/2012/
doi:10.5194/acpd-12-5881-2012
© Author(s) 2012. CC Attribution 3.0 License.

Atmospheric Chemistry and Physics Discussions

This discussion paper is/has been under review for the journal Atmospheric Chemistry and Physics (ACP). Please refer to the corresponding final paper in ACP if available.

Quantifying population exposure to airborne particulate matter during extreme events in California due to climate change

A. Mahmud, M. Hixson, and M. J. Kleeman

Department of Civil and Environmental Engineering, University of California at Davis, One Shields Ave, Davis CA 95616, USA

Received: 14 December 2011 – Accepted: 7 February 2012 – Published: 23 February 2012

Correspondence to: M. J. Kleeman (mjkleeman@ucdavis.edu)

Published by Copernicus Publications on behalf of the European Geosciences Union.

Abstract

The effect of climate change on population-weighted concentrations of particulate matter (PM) during extreme events was studied using the Parallel Climate Model (PCM), the Weather Research and Forecasting (WRF) model and the UCD/CIT 3-D photochemical air quality model. A "business as usual" (B06.44) global emissions scenario was dynamically downscaled for the entire state of California between the years 2000–2006 and 2047–2053. Air quality simulations were carried out for 1008 days in each of the present-day and future climate conditions using year-2000 emissions. Population-weighted concentrations of $PM_{0.1}$, $PM_{2.5}$, and PM_{10} total mass, components species, and primary source contributions were calculated for California and three air basins: the Sacramento Valley air basin (SV), the San Joaquin Valley air basin (SJV) and the South Coast Air Basin (SoCAB). Results over annual-average periods were contrasted with extreme events.

Climate change between 2000 vs. 2050 did not cause a statistically significant change in annual-average population-weighted $PM_{2.5}$ mass concentrations within any major sub-region of California in the current study. Climate change did alter the annual-average composition of the airborne particles in the SoCAB, with notable reductions of elemental carbon (EC; −3 %) and organic carbon (OC; −3 %) due to increased annual-average wind speeds that diluted primary concentrations from gasoline combustion (−3 %) and food cooking (−4 %). In contrast, climate change caused significant increases in population-weighted $PM_{2.5}$ mass concentrations in central California during extreme events. The maximum 24-h average $PM_{2.5}$ concentration experienced by an average person during a ten-year period in the SJV increased by 21 % due to enhanced production of secondary particulate matter (manifested as NH_4NO_3). In general, climate change caused increased stagnation during future extreme pollution events, leading to higher exposure to diesel engines particles (+32 %) and wood combustion particles (+14 %) when averaging across the population of the entire state. Enhanced stagnation also isolated populations from distant sources such as shipping

ACPD

12, 5881–5901, 2012

(−61 %) during extreme events. The combination of these factors altered the statewide population-averaged composition of particles during extreme events, with EC increasing by 23 %, nitrate increasing by 58 %, and sulfate decreasing by 46 %.

1 Introduction

Air pollution is a persistent public health problem in the United States with over 158 million people living in regions that violate the National Ambient Air Quality Standards (NAAQS) (USEPA, 2008). The pollutant of greatest health concern is airborne particulate matter with aerodynamic diameter smaller than 2.5 µm ($PM_{2.5}$). Epidemiological studies have estimated rates of mortality and morbidity associated with $PM_{2.5}$ (see for example, Samet et al., 200; Doeckery et al., 1993; Pope et al., 1995) yielding predictions that an average of 24 000 people die from exposure to particulate matter each year in the United States (Mokdad et al., 2005). California experiences a disproportionately large fraction of these deaths (Tran et al., 2008) because it is home to two of the air basins that experience some of the highest $PM_{2.5}$ concentrations each year. The South Coast Air Basin (SoCAB) has ∼15 million residents that experience 24-h average $PM_{2.5}$ concentrations that are up to ∼2.3 times higher than the NAAQS. The San Joaquin Valley (SJV) has ∼3 million residents that experience 24-h average $PM_{2.5}$ concentrations that exceed the NAAQS by a factor of ∼2.3 (24-h average).

Meteorology plays an important role in California's air pollution problems. Persistent stagnation events develop when high pressure systems stall over the air basins trapping leading to reduced ventilation of emissions. Temperature, wind speed, wind direction, and mixing height in the atmosphere play critical roles in determining patterns of air quality over multiple scales of time and space by affecting emissions, atmospheric transformation, and deposition of particles (Kinney et al., 2008). Global climate change is likely to alter these meteorological parameters affecting air quality (see for example, Kleeman, 20008; Aw and Kleeman, 2003; Sillman et al., 1995) with unknown consequences to human health.

ACPD
12, 5881–5901, 2012

Recently Tagaris et al. (2009) investigated the potential impact of climate change on $PM_{2.5}$ related health effects for the United Stated using the Environmental Protection Agency (EPA's) Environmental Benefits Mapping and Analysis Program (BenMAP). The authors showed that the national average premature mortality is likely to increase by 4000 cases in 2050 compared to 2001 along with both increasing and decreasing mortality trends in different states due to climate change alone. California was predicted to experience an average decrease of 186 cases of premature death with decreasing trends also predicted for other $PM_{2.5}$-related health issues including chronic and acute bronchitis, asthma, hospital admissions, and respiratory diseases in the future. This health effects analysis was a valuable first estimate but it was based on a discrete set of simulations that had limited ability to characterize the inter-annual variability that drives the uncertainty in annual-average exposure periods or the extreme events that drive the uncertainty in the 24-h average exposure periods.

The objective of the current study is to quantify the impact of climate change on population-weighted concentrations of $PM_{0.1}$, $PM_{2.5}$, and PM_{10} mass in California over annual averages and during extreme 24-h periods. The analysis is based on more than 1000 simulated days of present climate and 1000 simulated days of future climate with 8-km spatial resolution that span enough years to capture inter-annual variability associated with large scale patterns such as El Nino Southern Oscillation (ENSO) cycles. The large number of simulation days also provides enough information about the tails of the distribution to support a rigorous analysis of extreme events. The results are put into proper context by quantifying the magnitude of the climate effect relative to the uncertainty in the analysis.

1.1 Methods

The impact of climate change on regional air quality over the entire state of California was studied using the Parallel Climate Model (PCM), the Weather Research and Forecasting (WRF) model, and the latest generation of the UCD/CIT air quality model. A schematic diagram and detailed description of the modeling system is presented

ACPD
12, 5881–5901, 2012

elsewhere (Mahmud et al., 2010). An overview of the modeling system is presented below.

PCM (Washington et al., 2000) data generated under the "business as usual" (B06.44) global emissions scenario was dynamically downscaled to 4-km resolution using the WRF model version 2.2 (Skamarock, 2004) for present-day (2000–2006) and future (2047–2053) time periods. The original PCM dataset was generated for a continuous period from 1995 to 2099 with CO_2 increasing by 1 % per year. The WRF model was optimized for California simulations with the physics schemes described by Mahmud et al. (2010). A total of 153 days equally divided into nine periods of 17 days each were simulated for each year. Gaps of 25 days were left between simulation periods to evenly distribute the active days starting on 1 January throughout the year. This pattern captures an unbiased sample of 1008 days over each of the seven-year periods. The WRF 4-km fields were averaged to 8-km for the air quality simulations to increase the speed of the calculations without sacrificing significant accuracy in the final results (see for example Ying et al., 2008). The final air quality modeling domain was composed of 131 × 128 × 10 grid cells (x-y-z) spanning the entire state of California with a first vertical height of 30 m and a total vertical depth of 5 km above ground.

The base-case raw emissions inventories for the year 2000 were obtained from the California Air Resources Board (CARB) and the South-Coast Air Quality Management District (SCAQMD). Emissions for both the future and present-day simulations were kept at year 2000 levels so that the results directly quantify the effect of changing climate and background concentrations. On-road mobile source emissions and biogenic volatile organic emissions were adjusted for the variation of meteorological conditions experienced during each simulation using CARB's Emissions Factors (EMFAC) model, and biogenic processing model (BEIGIS), respectively. The techniques to adjust these emissions are summarized by Mahmud et al. (2010). Source-oriented and gridded hourly emissions were generated by merging the adjusted on-road mobile and biogenic sources with the original area and point source emissions. Seasonally variable initial conditions (ICs) and boundary conditions (BCs) of gas-phase and particle-phase

ACPD
12, 5881–5901, 2012

species were specified for the air quality model calculations. A summary of the ICs and BCs is provided by Mahmud et al. (2010).

The source oriented UCD/CIT 3-D photochemical model (see for example, Ying et al., 2008; Held et al., 2004; Kleeman and Cass, 2001; Kleeman et al., 1997; Mysliwiec and Kleeman, 2002; Ying and Kleeman, 2003, 2006) was updated in the current study (Mahmud et al., 2010) with a scheme to re-calculate vertical wind to enforce mass conservation. The fully dynamic treatment of gas-particle conversion using the Aerosol Inorganic Module (AIM) thermodynamic code (Wexler and Seinfeld, 1992) was replaced by the approach proposed by Jacobson (2005) using the ISORROPIA II thermodynamics package (Fountoukis and Nenes, 2007; Nenes et al., 1998) to calculate the vapor pressure of semi-volatile inorganic species above each particle surface. The revised model also includes a new wet deposition scheme and a sea salt emissions scheme.

Figure 1 shows the air quality modeling domain and three air basins of interest: the Sacramento Valley air basin (SV), the San Joaquin Valley air basin (SJV) and the South Coast Air Basin (SoCAB). Population-weighted concentrations of particles were calculated for these air basins and for the entire state of California so that the impacts of climate change on public health via changes to air quality could be viewed more directly. According to the 2000 census California has a total population of 33.9 million, with a total land area of 4.24×10^5 km^2. The population of the SV was 2.4 million with an area of 0.38×10^5 km^2, the population of the SJV was 3.2 million with an area of 0.60×10^5 km^2, and the population of the SoCAB was 14.6 million with an area of 0.18×10^5 km^2. The population density and population spatial distribution were held constant at year 2000 census values in all present and future year simulations to be consistent with the assumption of constant emissions. This approach produces results that directly illustrate the effects of climate change without confounding factors. The population-weighted concentration is calculated as $\sum_{i=1}^{n} \frac{p_i \times C_i}{p_{\text{tot}}}$, where i designates each computational cell in the domain, p_i is the population at a given cell location, C_i is the

ACPD
12, 5881–5901, 2012

particulate concentration in the same cell location, and p_{tot} is the total population in the domain of interest (i.e. air basin wide total population).

PM concentrations averaged over 24-h periods were analyzed using the open source statistical software R version 2.10.0 with the University Cooperation for Atmospheric Research (UCAR) extremes toolkit version 1.62. Data from the present-day (2000–2006) and future (2047–2053) were analyzed separately, and the climate change impact was quantified by taking the difference between them. The 10-yr return level and its associate parameters were calculated based on the Generalized Pareto Distribution (GPD) probability model first introduced by Pickands (1975). In this method, the extreme values greater than some threshold are typically assumed to have the following density function:

$$F(x;k;\sigma) = \begin{cases} 1-\left(1-\frac{kx}{\sigma}\right)^{\frac{1}{k}}; k \neq 0, \sigma > 0 \\ 1-\exp\left(-\frac{x}{\sigma}\right); k = 0, \sigma > 0 \end{cases} \quad (1)$$

where k and σ are shape and scale parameters with x in the range of $x > 0$ for $k \leq 0$ and $0 < x < \sigma/k$ for $k > 0$. There has been a great interest in applying the GPD model to analyze extreme events in environmental datasets (see for example, Brabson et al., 2000; Pisarenko and Sornette, 2003; Li et al., 2005; Jagger et al., 2006; Coles and Tawn, 1991; Coles, 2001) . The threshold value for each variable of interest in both the present-day and future datasets was chosen based on the distribution of all data points, which was approximately equivalent to the 3rd quantile value of the ranked dataset. The 90 % confidence intervals (CI) of 10-yr return levels were also calculated in this study.

1.2 Results

Table 1 summarizes the population-weighted annual average concentrations of $PM_{2.5}$ total mass, component species, and primary sources for the present-day (2000–2006). The highest calculated population-weighted annual $PM_{2.5}$ total mass concentration

ACPD
12, 5881–5901, 2012

was ~11 μg m^{-3} in the SoCAB followed by ~8 μg m^{-3} in the SJV and ~7 μg m^{-3} in the SV. Population-weighted total mass concentration for the entire state of California was ~9 μg m^{-3}. Organic carbon (OC) (mostly primary) is the major component of this total mass (~24 %), followed by secondary nitrate (~14 %). Dust is the major contributor to the total primary mass followed by wood smoke, meat cooking, miscellaneous, diesel combustion, high sulfur content fuels, gasoline combustion, and shipping.

1.2.1 Annual average PM concentrations

The differences between future (2047–2053) and present-day (2000–2006) population-weighted annual average concentrations of $PM_{2.5}$ are displayed in Fig. 2 for the entire state of California and the three major air basins highlighted in Fig. 1. Concentrations of total mass, major components, and primary particle source categories were calculated. The error bars in these figures represent 90 % confidence intervals for the mean difference based on the inter-annual variability within each analysis period.

Population-weighted annual average concentrations of $PM_{2.5}$ total mass were predicted to decrease by ~2 % from the present-day conditions in the SoCAB with little change predicted for the SV and SJV. Concentrations of all major $PM_{2.5}$ components such as elemental carbon (EC), organic carbon (OC), sulfate (S(VI)), and ammonium ion (N(-III)) followed this downward trend. In contrast, statewide population-weighted concentrations of $PM_{2.5}$ nitrate (N(V)) increased by ~2 %. Population-weighted primary $PM_{2.5}$ concentrations from all sources including dust, shipping, wood smoke, diesel combustion, gasoline combustion, meat cooking, high sulfur content fuels, and miscellaneous were predicted to decrease by between ~2–6 % in California in the future.

Figures S1 and S2 in the supporting information section present the analysis illustrated for Fig. 2 for the $PM_{0.1}$ and PM_{10} size fractions with largely the same conclusion that the future analysis period tends to have lower annual-average population-weighted concentrations than the present-day analysis period.

Uncertainty analysis must be considered to put the results illustrated in Fig. 2 into proper context. The error bars in this figure represent the 90 % confidence interval

ACPD
12, 5881–5901, 2012

based on the inter-annual variability within each analysis period. The most significant feature displayed in this figure is the size of the uncertainty bars induced by inter-annual variability vs. the size of the average change between future and present years. In the majority of cases, the magnitude of the inter-annual variability is greater than the average change between future and present years. For example, the 90 % CI for climate-induced change to statewide population-averaged $PM_{2.5}$ concentrations ranges from −6 % to 2 % making it statistically identical to zero. The only exception to this trend is a 4 % (90 %CI: −7.5 % to −0.5 %) reduction in OC concentrations caused by reduced contributions from primary combustion sources such as gasoline combustion (−3 %) and meat cooking (−4 %) in the SoCAB.

The fact that 90 % confidence intervals displayed in Fig. 2 (also in Figs. S1 and S2) largely overlap zero implies that a random selection of different years within each climate period could lead to either positive or negative effects on concentrations. The Intergovernmental Panel on Climate Change (IPCC) Third Assessment Report (AR3) (2001) and the Fourth Assessment Report (AR4) (2007) projected future global changes relative to the present-day based on 30-yr (1960–1989) and 20-yr (1980–1999) averages, respectively. In the current study, only ∼40 % of the days within seven-year periods in the present-day (2000–2006) and future (2047–2053) were simulated. The reduced analysis window greatly lowers the computational burden of the problem while still capturing the inter-annual variability associated with the ENSO cycle. Unfortunately, the limited number of sample points also increase the uncertainty of the comparison between present-day and future climate since the uncertainty range in the comparison is inversely proportional to the square root of n (= number of simulated days). The current results span more days of air quality in California than any previous study and so they provide a best estimate for the effect of climate on annual-average population-weighted PM concentrations in California. Even with 1008 simulated days, the length of the analysis periods must be expanded to calculate a full set of statistically significant changes.

ACPD
12, 5881–5901, 2012

It must also be recognized that the inter-annual variability is only one source of uncertainty in the climate-air quality calculation. Most notably, the uncertainties introduced by the choice and configuration of the GCM, RCM, and air quality models are not included in the current analysis (or any previous analysis). Running a complete ensemble of calculations over a full 20-yr analysis period would fully characterize this uncertainty, but this effort was beyond the scope of the current study.

1.2.2 Extreme events

The frequency distributions of population-weighted daily-average $PM_{2.5}$ total mass concentrations have similar shapes for the 1008 days of present climate and the 1008 days of future climate (Fig. S3), but the upper tails of these distributions exhibit different behavior. Notably, the extreme concentration events defined to be the highest 1 % of the predicted concentrations (99th percentile) range from 16.5–19.2 $\mu g\,m^{-3}$ in the present climate and 16.6–24.7 $\mu g\,m^{-3}$ in the future climate. Short-term extreme concentrations of $PM_{0.1}$, $PM_{2.5}$ and PM_{10} have public health implications through acute mortality or through their contributions to chronic exposure. Further analysis was carried out to understand the effects of climate change on extreme PM concentrations in California.

Figure 3 shows the average $PM_{2.5}$ total mass concentrations corresponding to the 10 days with the highest population-weighted $PM_{2.5}$ concentrations in California (99th percentile extreme concentrations). Panel (a) shows the 10-day average concentrations for the future extreme events (2047–2053), panel (b) shows the 10-day average concentrations for the present-day extreme events (2000–2006), and panel (c) shows the difference between the future and present-day extreme events.

Extreme events in the future climate are characterized by 99th percentile $PM_{2.5}$ concentrations of ~45–55 $\mu g\,m^{-3}$ around cities including Bakersfield, Fresno, and Sacramento (panel a). In comparison, extreme events in the present climate exhibit 99th percentile $PM_{2.5}$ concentrations in the range between ~35–45 $\mu g\,m^{-3}$ around major cities (panel b). The extreme concentrations exceed both the California Ambient Air

ACPD
12, 5881–5901, 2012

Quality Standard (CAAQS) of 20 $\mu g\,m^{-3}$ and the National Ambient Air Quality Standard (NAAQS) of 35 $\mu g\,m^{-3}$ for 24-h average $PM_{2.5}$ total mass concentration. Panel (c) shows that the extreme 99th percentile concentrations are predicted to increase by ~15–19 $\mu g\,m^{-3}$ in and around Bakersfield, Fresno, Sacramento, and San Francisco in the future climate compared to present-day. The maximum future increase of ~18–20 $\mu g\,m^{-3}$ is predicted to occur in areas between Fresno and Bakersfield in the SJV. Extreme $PM_{2.5}$ concentrations in Los Angeles are predicted to decrease by ~2 $\mu g\,m^{-3}$ in the future with larger decreases of ~15 $\mu g\,m^{-3}$ predicted in Ventura county west of Los Angeles.

Further statistical analysis was carried out for $PM_{0.1}$, $PM_{2.5}$ and PM_{10} population-weighted 24-h average concentrations based on extreme value theory (EVT) (Coles, 2001), which included more data points in order to relax the constraint imposed by the 99th percentile values used in the previous analysis. Figure 4 displays the change in the population-weighted ten-year return level for 24-h average $PM_{2.5}$ concentrations due to climate change between 2000 and 2050. Simply stated, this is the change in maximum 24-h average $PM_{2.5}$ concentration that an average person would experience in a decade due to climate change. The error bars shown in Fig. 4 represent the lower and upper limits of the 90 % confidence intervals.

The 10-yr return levels for $PM_{2.5}$ EC (+23 %) and NO_3^- (+58 %) averaged over the statewide population were predicted to increase in the future while statewide 10-yr return levels for $PM_{2.5}$ SO_4^{2-} (−46 %) were predicted to decrease. These trends reflect increased stagnation during future pollution events which traps pollutants close to their emissions source and provides greater time for the formation of secondary products. Statewide contributions to primary $PM_{2.5}$ from diesel engines (+32 %) and wood burning (+14 %) increase during future extreme pollution events while contributions from off-shore shipping (−61 %) decrease. Effects during extreme events were felt most strongly in the SJV, producing an increase of 21 % in the 10-yr return level for population-weighted $PM_{2.5}$ mass in that region, mostly due to increased concentrations of primary OC and enhanced formation of NH_4NO_3 during the future extreme

ACPD
12, 5881–5901, 2012

stagnation events. The change in the 10-yr return levels for PM_{10} and $PM_{0.1}$ (Figs. S4 and S5) are qualitatively similar to $PM_{2.5}$ results.

2 Discussion

The effects of climate change on airborne PM mass concentrations in California between the years 2000–2006 and 2047–2053 are generally smaller than the natural inter-annual variability within either of these periods. Population-weighted concentrations of $PM_{0.1}$/$PM_{2.5}$/PM_{10} mass in the SoCAB, SJV, SV, and across the entire state were not statistically different in the future climate vs. the present climate even though 1008 representative days were simulated in each climate period. Likewise, concentrations of PM chemical components and primary source contributions generally did not respond to climate change in a statistically significant fashion other than a few notable exceptions discussed below. The results of these tests are unable to reject the hypothesis that climate change has only a small effect on annual-average population-weighted airborne PM mass in California's major air basins. This implies that any calculation that combines the population-weighted concentrations from <1000 sample days with mortality or morbidity coefficients derived from epidemiological studies would likewise be unable to find statistically significant effects of climate change on human health due to changes in annual-average airborne PM mass. Caution must be used when interpreting the results from recent studies that show projected health benefits of climate change via changes to airborne PM in California.

Climate change did alter the annual-average composition of the airborne particles in the SoCAB, with notable reductions of elemental carbon (EC; −3 %) and organic carbon (OC; −3 %) due to increased annual-average wind speeds that diluted primary concentrations from gasoline combustion (−3 %) and food cooking (−4 %). These trends reflect the increase in annual-average wind speed over coastal portions of California. Future epidemiology studies may be able to quantify health effects associated with changes to individual PM chemical components and/or sources.

ACPD
12, 5881–5901, 2012

An analysis of extreme pollution events suggests that sub-regions of California will experience increased 99th percentile values of population-weighed concentrations as well as higher 10-yr return levels of primary PM due to climate change. Changes to the source contributions and composition of particles during extreme events are significant when averaged over the population of the entire state. These trends are consistent with the increased strength of future stagnation events which trap pollutants close to the emissions source. Stronger stagnation events increase population-weighted extreme concentrations of emissions released close to major cities and decrease the effects of more remote sources. The public health consequences of increased concentrations during extreme events are difficult to predict. Assuming that the same susceptible populations respond to long-term exposure and extreme events, then the relevant public health indicator is likely increased concentrations in either exposure category. If different susceptible populations respond to long-term exposure and extreme events, then decreases in one type of exposure will offset the effects of increases in the other exposure. Future epidemiological studies will need to consider these issues in light of the competing climate trends for annual-average vs. extreme PM concentrations in California.

Supplementary material related to this article is available online at: http://www.atmos-chem-phys-discuss.net/12/5881/2012/acpd-12-5881-2012-supplement.pdf.

Acknowledgements. This research was funded by the California Air Resources Board under Contract # 04-349. The statements and conclusions of this report are those of the contractor and not necessarily those of the California Air Resources Board. The mention of commercial products, their source, or their use in connection with material reported herein is not to be construed as actual or implied endorsement of such products.

ACPD
12, 5881–5901, 2012

References

Aw, J. and Kleeman, M. J.: Evaluating the first-order effect of intraannual temperature variability on urban air pollution, J. Geophys. Res., 108, D12, doi:10.1029/2002JD002688, 2003.

Brabson, B. B. and Palutikof, J. P.: Tests of the Generalized Pareto Distribution for Predicting Extreme Wind Speeds, J. Appl. Meteorol., 39, 1627–1640, 2000.

Coles, S. G. and Tawn, J. A.: Modelling extreme multivariate events, J. Roy. Stat. Soc. B, 53, 377–392, 1991.

Coles, S.: An introduction to statistical modeling of extreme values, Springer, 2001.

Dockery, D. W., Arden Pope, C., Xu, X., Spengler, J. D., Ware, J., H., Fay, M. E., Ferris Jr., B. G., and Speizer, F. E.: An Association between Air-Pollution and Mortality in 6 United-States Cities, New Engl. J. Med., 329, 1753–1759, 1993.

Fountoukis, C. and Nenes, A.: ISORROPIA II: a computationally efficient thermodynamic equilibrium model for K^+ Ca^{2+} Mg^{2+} NH^{4+} Na^+ SO_4^{2} NO_3^- Cl^- H_2O aerosols, Atmos. Chem. Phys., 7, 4639–4659, doi:10.5194/acp-7-4639-2007, 2007.

Held, T., Ying, Q., Kaduwela, A., and Kleeman, M.: Modeling particulate matter in the San Joaquin Valley with a source-oriented externally mixed three-dimensional photochemical grid model, Atmos. Environ., 38, 3689–3711, 2004.

Jacobson, M. Z.: A solution to the problem of nonequilibrium acid/base gas-particle transfer at long time step, Aerosol Sci. Technol., 39, 92–103, 2005.

Jagger, T. H. and Elsner, J. B.: Climatology models for extreme hurricane near the United States, J. Climate, 19, 3220–3236, 2006.

Kinney, P. L.: Climate Change, Air Quality, and Human Health, Am. J. Prev. Med., 35, 459–467, 2008.

Kleeman, M. J.: A preliminary assessment of the sensitivity of air quality in California to global change, Climatic Change, 87, S273–S292, 2008.

Kleeman, M. J., Cass, G. R., and Eldering, A.: Modeling the airborne particle complex as a source-oriented external mixture, J. Geophys. Res. Atmos., 102, 21355–21372, doi:10.1029/97JD01261, 1997.

Kleeman, M. J. and Cass, G. R.: A 3D Eulerian source-oriented model for an externally mixed aerosol, Environ. Sci. Technol., 35, 4834–4848, 2001.

Li, Y., Cai, W., and Campbell, E. P.: Statistical modeling of extreme rainfall in southwest Western Australia, J. Climate, 18, 852–863, 2005.

ACPD
12, 5881–5901, 2012

Mahmud, A., Hixson, M., Hu, J., Zhao, Z., Chen, S.-H., and Kleeman, M. J.: Climate impact on airborne particulate matter concentrations in California using seven year analysis periods, Atmos. Chem. Phys., 10, 11097–11114, doi:10.5194/acp-10-11097-2010, 2010.
Mokdad, A.H., Marks, J. S., Stroup, D. F., and Gerberding, J. L.: Actual causes of death in the United States, 2000, J. Amer., Med. Assoc., 291, 1238–1245, 2004.
Mysliwiec, M. J. and Kleeman, M. J.: Source apportionment of secondary airborne particulate matter in a polluted atmospbere, Environ. Sci. Technol., 36, 5376–5384, 2002.
Nenes, A., Pandis, S. N., and Pilinis, C.: ISORROPIA: A new thermodynamic equilibrium model for multiphase multicomponent inorganic aerosols, Aquat. Geochem., 4, 123–152, 1998.
Pickands, J.: Statistical Inference Using Extreme Order Statistics, Ann. Stat., 3, 119–131, 1975.
Pisarenko, V. F. and Sornette, D.: Characterization of the frequency of extreme earthquake events, Pure Appl. Geophys., 160, 2343–2364, 2003.
Pope 3rd, C. A., Thun, M. J., Namboodiri, M. M., Dockery, D. W., Evans, J. S., Speizer, F. E., and Heath Jr., C. W.: Particulate Air-Pollution as a Predictor of Mortality in a Prospective-Study of Us Adults, Am. J. Respir. Crit. Care Med., 151, 669–674, 1995.
Samet, J. M., Dominici, F., Curriero, F. C., Coursac, I., and Zeger, S. L.: Fine particulate air pollution and mortality in 20 US Cities, 1987–1994, New Engl. J. Med., 343, 1742–1749, 2000.
Sillman, S. and Samson, F. J.: Impact of Temperature on Oxidant Photochemistry in Urban, Polluted Rural and Remote Environments, J. Geophys. Res.-Atmos., 100, 11497–11508, 1995.
Skamarock, W. C.: Evaluating mesoscale NWP models using kinetic energy spectra, Mon. Weather Rev., 132, 3019–3032, 2004.
Tagaris, E., Liao, K. J., Delucia, A. J., Deck, L., Amar, P., and Russell, A. G.: Potential Impact of Climate Change on Air Pollution-Related Human Health Effects, Environ. Sci. Technol., 43, 4979–4988, 2009.
Tran, H. T., Alvarado, A., Garcia, C., Motallebi, N., Miyasato, L., and Vance, W.: Methodology for Estimating Premature Deaths Associated with Long-term Exposure to Fine Airborne Particulate Matter in California, California Environmental Protection Agency, Air Resources Board, Sacramento, CA, 2008.
United States Environmental Protection Agency (USEPA), Latest Findings on National Air Quality: Status and Trends through 2007, Office of the Air Quality Planning, 2008.

ACPD
12, 5881–5901, 2012

Washington, W. M., Weatherly, J. W., Meehl, G. A., Semtner, A. J., Bettge, T. W., Craig, A. P., Strand, W. G., Arblaster, J., Wayland, V. B., James, R., and Zhang, Y.: Parallel climate model (PCM) control and transient simulations, Clim. Dynam., 16, 755–774, 2000.

Wexler, A. S. and Seinfeld, J. H.: Analysis of Aerosol Ammonium-Nitrate – Departures from Equilibrium during Scaqs, Atmos. Environ. A-Gen., 26, 579–591, 1992.

Ying, Q. and Kleeman, M. J.: Effects of aerosol UV extinction on the formation of ozone and secondary particulate matter, Atmos. Environ., 37, 5047–5068, 2003.

Ying, Q. and Kleeman, M. J.: Source contributions to the regional distribution of secondary particulate matter in California, Atmos. Environ., 40, 736–752, 2006.

Ying, Q., Lu, J., Allen, P., Livingstone, P., Kaduwela, A., and Kleeman, M.: Modeling air quality during the California Regional PM10/PM2.5 Air Quality Study (CRPAQS) using the UCD/CIT source-oriented air quality model – Part I. Base case model results, Atmos. Environ., 42, 8954–8966, 2008.

ACPD

12, 5881–5901, 2012

Table 1. Population-weighted annual average concentrations ($\mu g\,m^{-3}$) of $PM_{2.5}$ total mass, major component species, metal and sources contributing to total primary mass for the present-day (2000–2006) for California (CA), and three air basins: Sacramento Valley (SV), San Joaquin Valley (SJV) and South Coast Air Basin (SoCAB). The error shown is one standard deviation.

Species/Category	CA	SV	SJV	SoCAB
Total mass	8.66 ± 0.39	7.22 ± 0.71	8.35 ± 0.78	10.9 ± 0.38
Elemental carbon (EC)	0.33 ± 0.02	0.34 ± 0.03	0.3 ± 0.02	0.38 ± 0.01
Organic carbon (OC)	2.04 ± 0.07	2.48 ± 0.23	1.66 ± 0.12	2.56 ± 0.04
Nitrate (N(V))	1.19 ± 0.15	0.87 ± 0.22	1.61 ± 0.32	1.56 ± 0.18
Sulfate (S(VI))	0.72 ± 0.05	0.47 ± 0.06	0.59 ± 0.06	0.87 ± 0.06
Ammonium (N(-III))	0.67 ± 0.06	0.47 ± 0.09	0.8 ± 0.11	0.85 ± 0.07
Trace metal (METL)	0.45 ± 0.02	0.33 ± 0.02	0.45 ± 0.03	0.59 ± 0.02
Dust	2.6 ± 0.1	1.65 ± 0.11	2.46 ± 0.18	3.47 ± 0.13
Shipping	0.09 ± 0	0 ± 0	0.01 ± 0	0.15 ± 0.01
Wood Smoke	0.86 ± 0.07	2.39 ± 0.24	1.52 ± 0.12	0.37 ± 0.03
Diesel Combustion	0.42 ± 0.02	0.39 ± 0.04	0.33 ± 0.03	0.56 ± 0.02
Gasoline Combustion	0.21 ± 0.01	0.1 ± 0.01	0.07 ± 0.01	0.37 ± 0.01
Meat Cooking	0.74 ± 0.02	0.13 ± 0.01	0.14 ± 0.01	1.4 ± 0.03
High Sulfur Content Fuels	0.23 ± 0.01	0.06 ± 0.01	0.07 ± 0.01	0.31 ± 0.01
Miscellaneous	0.62 ± 0.02	0.48 ± 0.04	0.51 ± 0.03	0.85 ± 0.02

ACPD
12, 5881–5901, 2012

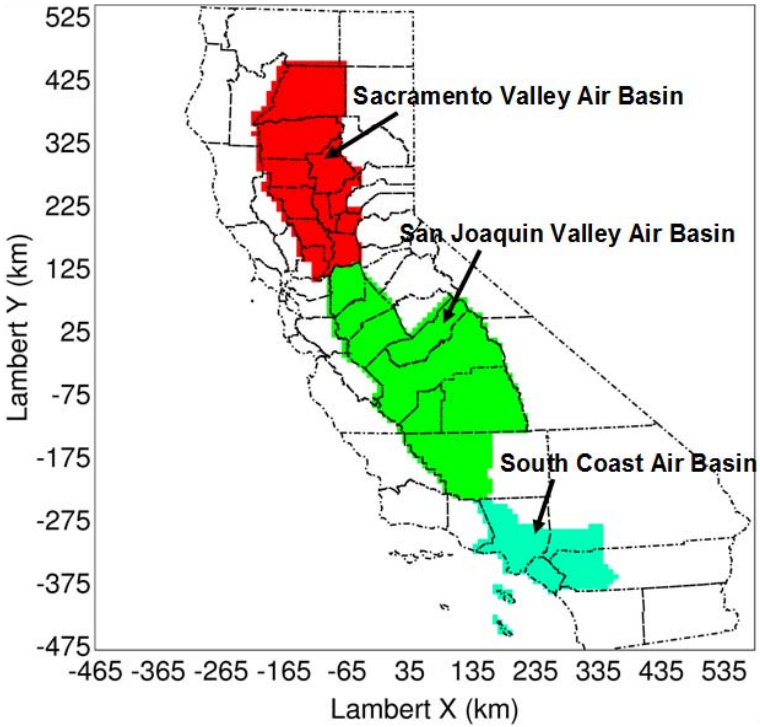

Fig. 1. Three major air basins in California: (1) Sacramento Valley Air Basin (SV), (2) San Joaquin Valley Air Basin (SJV), and (3) South Coast Air Basin (SoCAB). Note that the lines in the state map represents county boundaries in California.

ACPD
12, 5881–5901, 2012

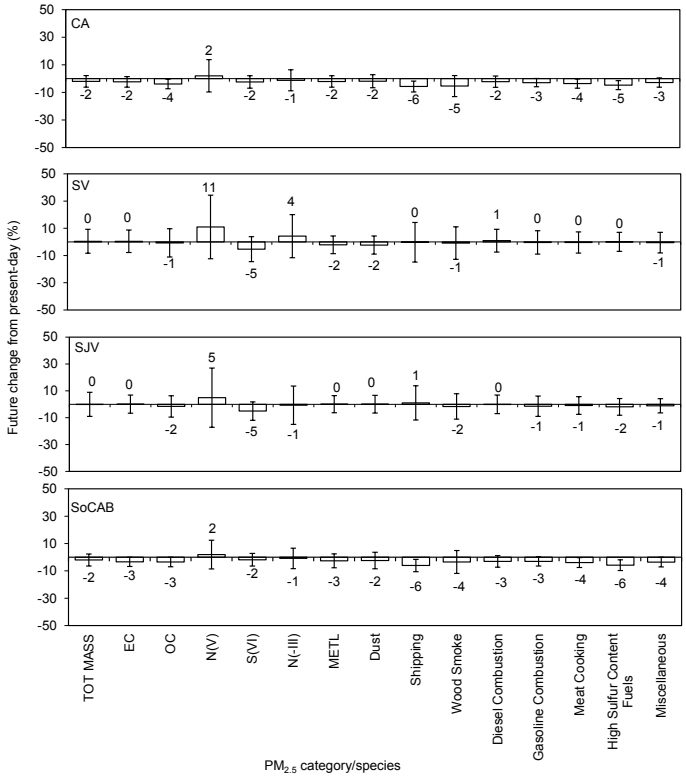

Fig. 2. Future (2047–2053) change in population-weighted annual-average concentrations of $PM_{2.5}$ total mass, primary and secondary components, and source categories contributing to the total mass from present-day (2000–2006). Panels (top-down) show California state-wide average, Sacramento Valley (SV) air basin average, San Joaquin Valley (SJV) air basin average, and South Coast Air Basin (SoCAB) average results. The error bars represent the 90 % CI.

ACPD
12, 5881–5901, 2012

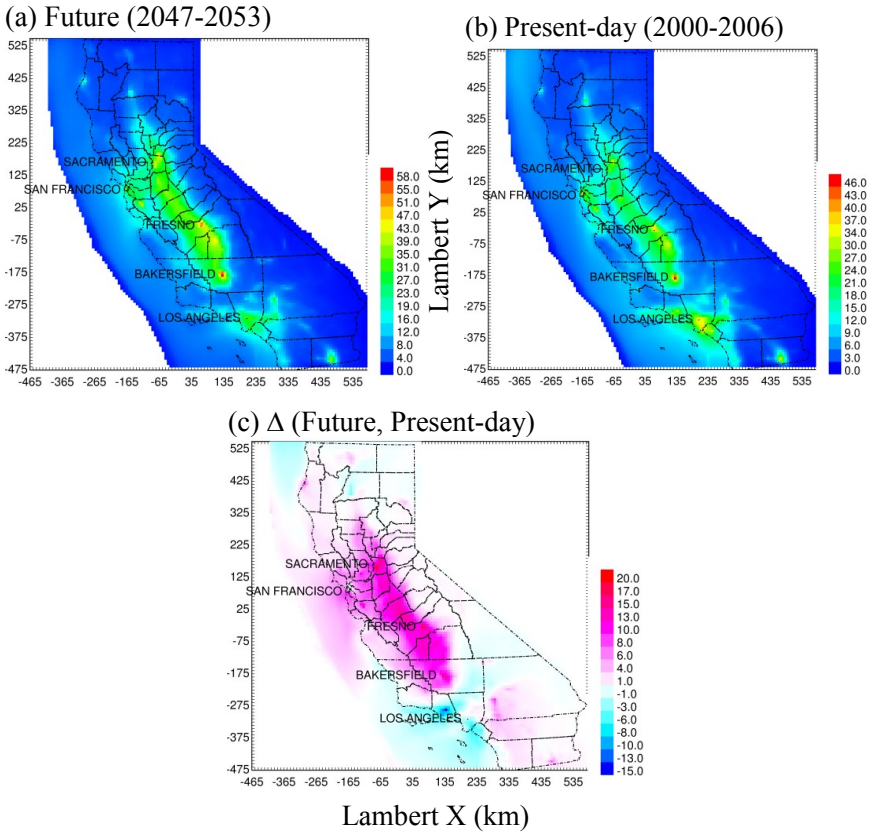

Fig. 3. Average of worst 24-h average $PM_{2.5}$ total mass concentrations ($\mu g\,m^{-3}$) corresponding to days with population-weighted concentrations above the 99th percentile values for California under the **(a)** future (2047–2053), and **(b)** present-day climate (2000–2006) conditions. Panel **(c)** shows the difference between the future **(a)** and present-day **(b)**.

ACPD
12, 5881–5901, 2012

Quantifying population exposure to airborne particulate matter

A. Mahmud et al.

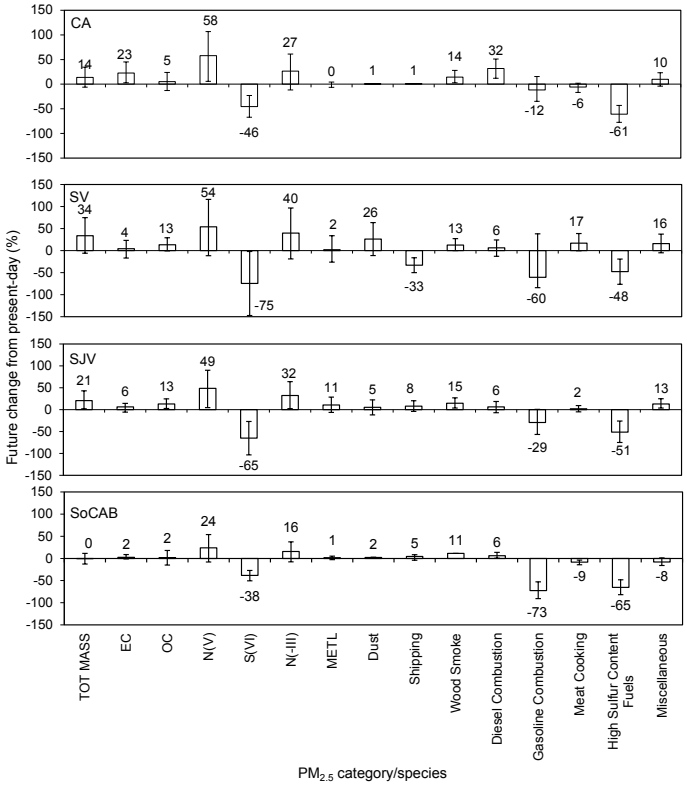

Fig. 4. Change in population-weighted extreme concentrations of $PM_{2.5}$ total mass, primary and secondary components, and source categories contributing to the total mass between future (2047–2053) and present-day (2000–2006). Values are the changes in the ten-year return levels which are the maximum 24-h average concentration experienced in a ten year period. Panels (top-down) show California state-wide average, Sacramento Valley (SV) air basin average, San Joaquin Valley (SJV) air basin average, and South Coast Air Basin (SoCAB) average results. The error bars represent the lower and upper limits of the 90 % CI.

ACPD
12, 5881–5901, 2012